Supporting Information

A multi-centre metal-free COF@g-C_3N_4 catalyst assembled with covalent bonds for photocatalytic CO_2 reduction

Xiang Wang[a], Zhenping Wang[a], Yanling Liu[a]*, Wanzhen Peng[a], Xiangyi Fu[a], Jie Zhou[a]*, Lizhi Han[a], Yingjie Hua[a] and Zi-Yan Zhou[b, c]*

[a] Key Laboratory of Electrochemical Energy Storage and Energy Conversion of Hainan Province, School of Chemistry and Chemical Engineering, Hainan Normal University, Haikou, Hainan, 571158, China.

[b] Shandong Engineering Research Center of Green and High-value Marine Fine Chemicals, Weifang University of Science and Technology, Shouguang, Shandong, 262700, China.

[c] College of Chemistry and Chemical Engineering, Shandong University of Technology, Zibo, 255000 Shandong, China.

*Correspondence and requests for materials should be addressed to Y. Liu (email: Liuyl7809@163.com), J. Zhou (email: 920486@hainnu.edu.cn) and Z.Y. Zhou (email: zyzhou@sdut.edu.cn).

Materials and methods

The starting materials for COF syntheses were purchased from Shanghai Tensus Bio-tech Co., Ltd. Other reagents and solvents applied in the synthesis and photocatalysis were purchased from Aladdin and Sigma-Aldrich, and used as received without further pretreatments.

The powder X-ray diffraction (PXRD) spectra were recorded on a D/max 2500 VL/PC X-ray diffractometer (Rigaku SmartLab, Japan) with Cu Kα radiation (λ = 1.5418 Å) at 45 kV, 200 mA. Diffraction intensity data for 2θ from 3 ~ 30° were collected at the scanning speed of 5 deg/min with 2θ step increment of 0.01°.

Fourier-transform infrared (FTIR) spectra were obtained from KBr pellets in a wavelength ranging from 4000-500 cm^{-1} on a Thermo Nicolet IS50 FTIR spectrometer.

UV–vis diffuse reflectance spectra (UV–vis DRS) were recorded at room temperature on a HITACHI U-4100 Spectrophotometer.

X-ray photoelectron spectroscopy (XPS) were recorded using a Escalab 250Xi instrument from Thermo Scientific equipped with an Al Kα microfocused X-ray source.

Nitrogen gas porosimetry measurements were performed on a automatic volumetric adsorption equipment using a (ASIQM0G002-3) and porosity analyzer after the samples were outgassed under a vacuum at 100 ℃ for 12 h. Apparent surface areas were determined using BET method.

The emission lifetime measurements were performed on an Edinburgh-State/Transient Fluorescence Spectrometer FLS1000 with an excitation wavelength at 340 nm.

Scanning electron microscope (SEM) images were performed on XL-30 ESEM-FEG. The elemental mappings of the samples were determined by EDX equipped on SEM with the type of Genesis 2000.

TEM and HRTEM images were recorded on aTalos F200i (Thermo Fisher Scientific, USA) transmission electron microscope at an accelerating voltage of 200 kV.

Thermogravimetric analysis of COFs powder samples was performed on a Diamond TG Thermal Analyzer System (Perkin-Elmer, USA) with heating rate of 10 ℃ min^{-1} from room temperature to 1000 ℃.

All the electrochemical measurements were conducted using CHI760E (Chenhua Co., China)electrochemical work-station.

Photocatalytic experiment and detection

In a quartz reactor (50 mL), the photocatalyst (10 mg), $CoCl_2$ (3 μmol) and bipyridine (bpy, 20 mg) were dispersed in in the solution containing acetonitrile, H_2O and triethanolamine (v:v:v = 8:1:1, 30 mL). This mixture system was bubbled with pure CO_2 gas for 15 min. The temperature of the reaction solution was maintained at 25 °C controlled by an outside flow of water during the reaction. Then, the system was irradiated under simulated sunlight using a 40W LED lamp with λ = 420 - 800 nm. Keeping the system airtight throughout the photocatalytic process.

The gaseous products were sampled by an off-line sampling syringe (0.5 mL) and then analysed by gas chromatography. To detect the yield of CO gas, gas (500 μL) in the middle of the test tube was collected using an off-line sampling syringe and injected into a gas chromatography system equipped with an FID detector using argon as the carrier gas. Retention time of CO was 1.8 min. To detect the formation of H_2, the gas (500 μL) of the test tube was transferred using an off-line sampling syringe and analysed by gas chromatography with TCD detector through a 5 Å molecular sieve column, with ultra-pure argon acting as both carrier and reference gas. Retention time of H_2 was 1.0 min. The volumes of the CO or H_2 produced were calculated by comparing the integrated areas of the signals of CO or H_2 with a calibration curve. The injector and detector temperatures were kept to be 60 °C.

Electrochemical measurements

All electrochemical characterisations including Mott-Schottky measurements, electrochemical impedance spectroscopy and photocurrent were tested using the following methods.[1, 2] Electrochemical measurements of COF@g-C_3N_4, COF-TpBb and g-C_3N_4 were conducted using a three-electrode electrochemical workstation system (CHI 760e). The ITO glass substrate (1 cm × 1 cm) was employed as the working electrode, the Pt wire as the auxiliary electrode and the Ag/AgCl electrode as the reference electrode. The samples (2 mg) were dispersed into the solution (1 mL) containing Nafion solution (100 μL, 0.5 wt%), water (450 μL), and ethanol (450 μL). After sonication, the spreading aqueous slurries were drop-cast onto the ITO glass substrate. Then, the working electrode was dried spontaneously under ambient temperature. 0.2 M Na_2SO_4 solution was used as the electrolyte. Irradiation was carried out by using a 40W LED lamp with 420-800 nm.

Synthesis of 1,4-Phenylenebis(thiourea)[3]

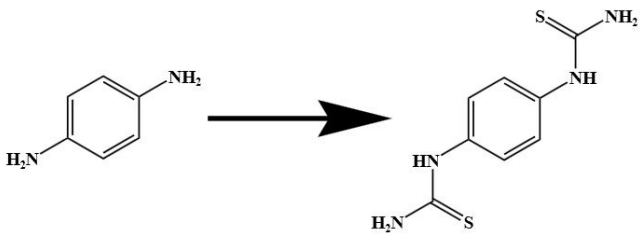

P-phenylenediamine (1.7 g, 15.7 mmol), activated carbon (1 g) and 3 mol L^{-1} hydrochloric acid (12 mL, 36 mmol) were added in a 100 mL three-necked flask. After being refluxed for 20 min, the mixture was filtered and the filtrate was removed into another 100 mL three-necked flask with ammonium thiocyanate (4.84 g, 63.6 mmol). After being heating at 95°C for 24 h, the solid product was collected by filtration and dried at 30°C in vacuum overnight.

Synthesis of 2,6-diaminobenzo[1,2-d:4,5-d′]bisthiazole (Bb-NH_2)[3]

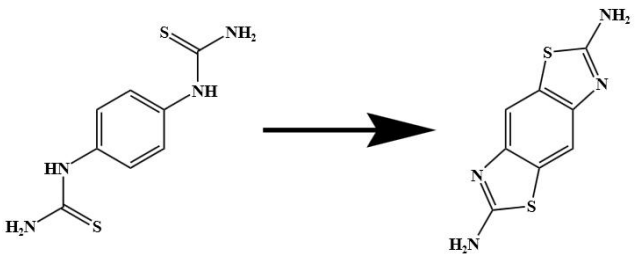

A solution of 1,4-Phenylenebis(thiourea) (2 g, 8.9 mmol) and trichloromethane (10 mL) were added into a 100 mL three-necked flask. Subsequently, a solution of trichloromethane (10 mL) containing liquid bromine (1.05 mL, 20.5 mmol) was added slowly into the mixture via a long-neck funnel, under stirring conditions. The temperature of the mixture was maintained at a maximum of 40 ℃. The suspension was stirred at room temperature for 12 h and refluxed for 24 h, then filtered and washed with trichloromethane (20 mL) for 4 times. The obtained solid and 20% sodium hydrogen sulfite solution (20 mL) were added into a 250 mL three-necked flask and stirred at 90°C. After filtration, the solid and 4 mol L^{-1} hydrochloric acid (25 mL, 100 mmol) were mixed and heated for 30 min. After filtration, the filtrate was neutralized with aqueous ammonia to pH = 7. The suspension was filtered and washed twice with methanol. The obtained solid was dried in vacuum at 35 ℃.

Synthesis of COF-TpBb

TpBb-COF was synthesized by the previously reported method with modification.[3, 4] A glass tube of 25 mL measuring 10 × 200 mm (o.d × length) was charged with Bb-NH_2 (33 mg, 0.15 mmol), Tp-CHO (21 mg, 0.1 mmol), 1,4-dioxane (0.75 mL), mesitylene (0.25 mL) and 6 M glacial acetic acid (0.1 mL). The mixture was sonicated for 30 min and then flash frozen in a liquid nitrogen bath at 77 K. After three freeze-pump-thaw cycles, the tube was sealed under vacuum and heated at 120ºC for 72 h under stationary condition. The precipitate at the bottom of the tube obtained from the reaction was collected by filtration, and then washed with dichloromethane and acetone, respectively. Finally, the product was dried at 100 ℃ under vacuum for 24 h to obtain a red solid as activated COF-TpBb.

Synthesis of g-C_3N_4

The synthesis of g-C_3N_4 was carried out using a previously reported method with slight modification.[5] The urea powder (10 g) was placed in a covered alumina crucible and heated to 550°C at a heating rate of 5°C·min^{-1} in a muffle furnace. The temperature was maintained for 4 h and then cooled to 25°C to obtain pure g-C_3N_4.

Synthesis of COF@g-C_3N_4-X

The COF@g-C_3N_4-0.2 composite photocatalyst was prepared as follows: the prepared COF-TpBb (20 mg) and g-C_3N_4 (80 mg) were ground for 30 min. The ground powder was dispersed in ethanol and water (v:v = 1:1, 50 mL) and stirring under room temperature for 12 h to form a suspension. Then, the suspension was transferred to a high-temperature and high-pressure resistant glass reactor (100 mL) and heated in an oven at 100 °C for 12 h. After naturally cooling down to room temperature, the pink powder was collected by vacuum filtration and washed thoroughly with distilled water and ethanol, and then dried at 100°C for 12 h under vacuum.

The synthesis procedure of COF@g-C_3N_4-X (X = 0.05/0.1/0.3) was the same as that of COF@g-C_3N_4-0.2, except that the mass of COF-TpBb:g-C_3N_4 = 1:4 were replaced by 1:19/1:9/3:7.

Computational methods

The calculation model is constructed by a finite cluster structure, and all calculations were performed with the Gaussian 16 software package. The ground state of [Cat.] was geometrically optimized by using 6-31G* basis sets. ESP analysis, TDDFT calculations, and orbital composition were also performed at the same level. In order to obtain the corresponding excited state energies, TDDFT calculations were performed on the basis of optimized ground state configurations. The energy of [Cat.] is specified as 0.000 eV, and the ΔE (eV) calculations for the other states.[6-8]

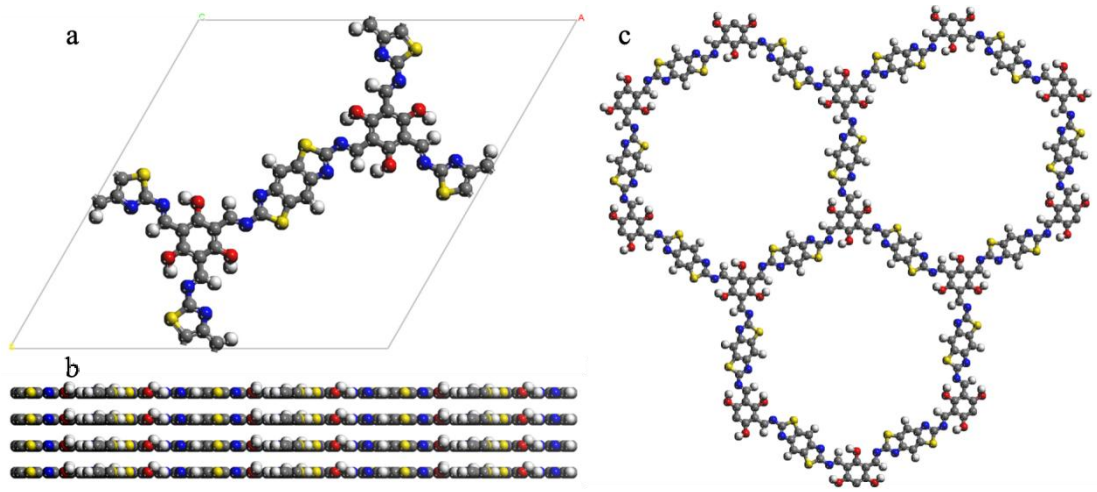

Figure S1. Space-filling model showing AA stacking: unit cell (a), side view (b) and top view (c); carbon (gray), nitrogen (blue), oxygen (red) and sulfur (yellow).

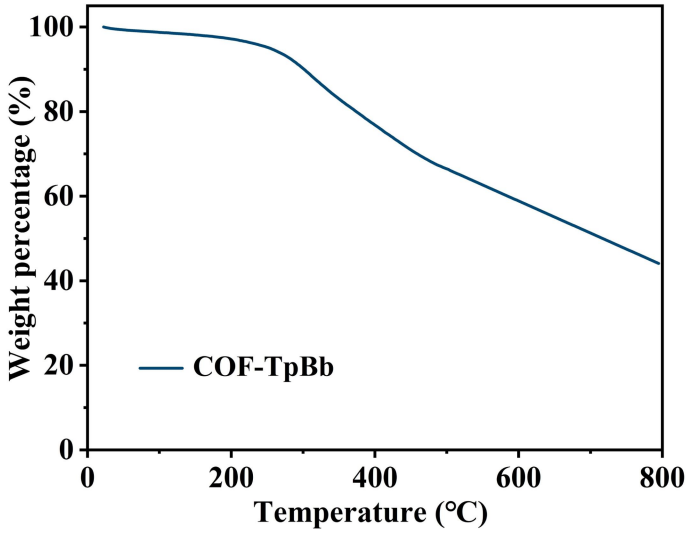

Figure S2. TGA curve of COF-TpBb under N_2 atmosphere.

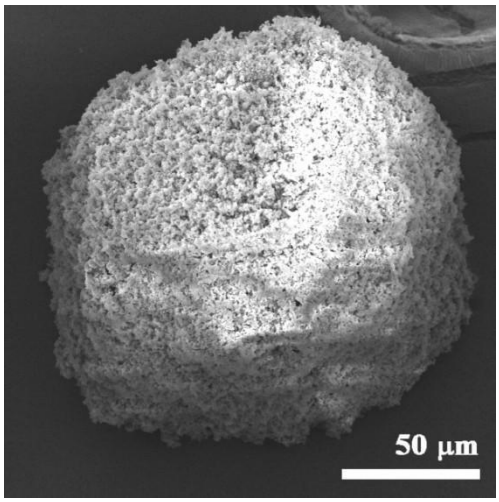

Figure S3. SEM images of Tp-CHO.

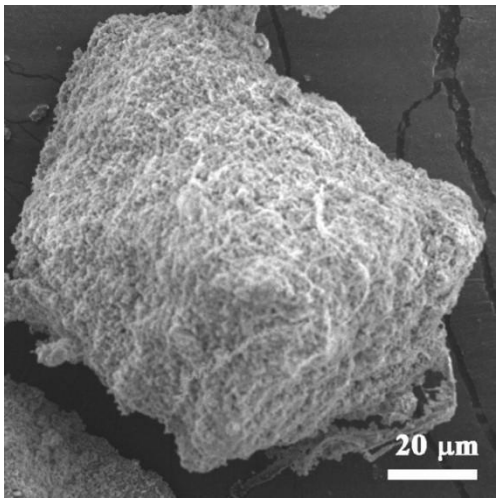

Figure S4. SEM images of Bb-NH_2.

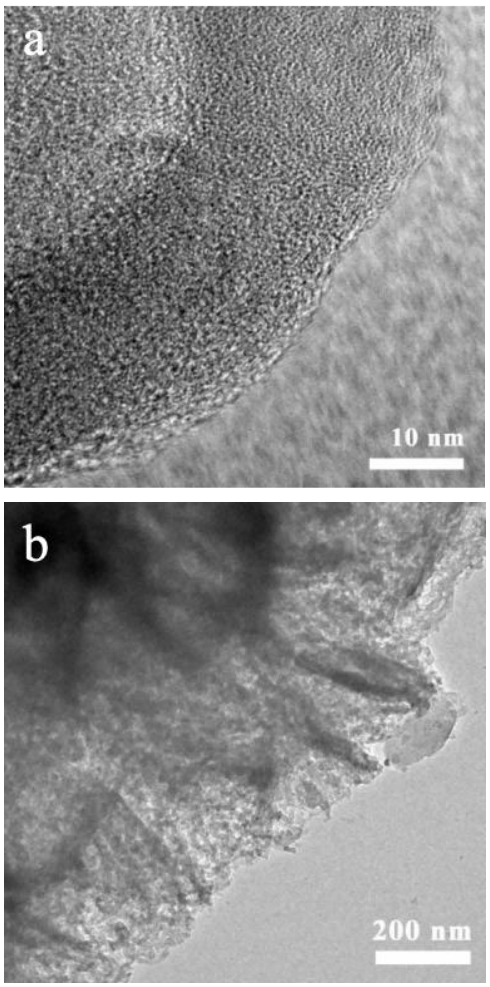

Figure S5. TEM images of COF-TpBb.**a** 10nm, **b** 200 nm.

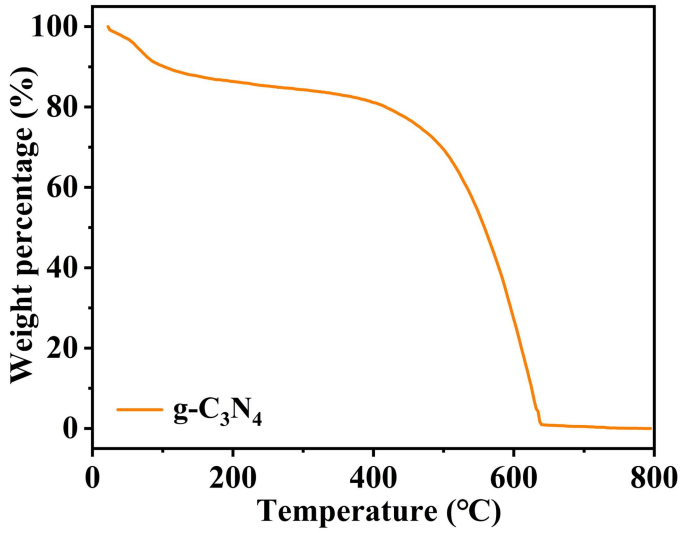

Figure S6. TGA curve of g-C_3N_4 under N_2 atmosphere.

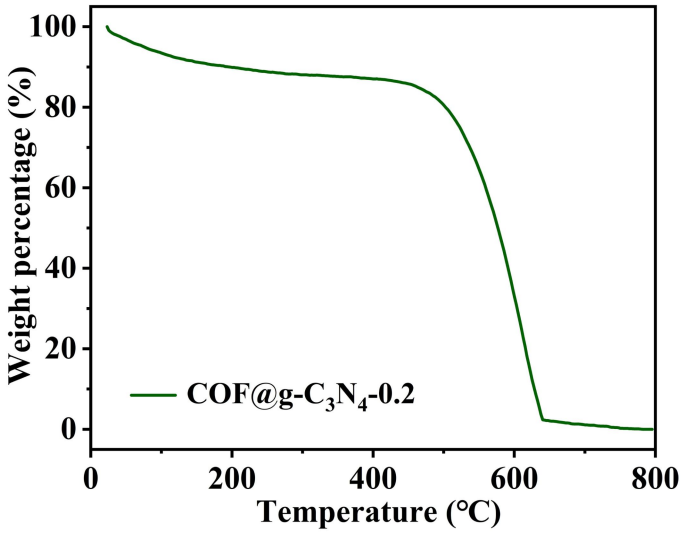

Figure S7. TGA curve of COF@g-C_3N_4-0.2 under N_2 atmosphere.

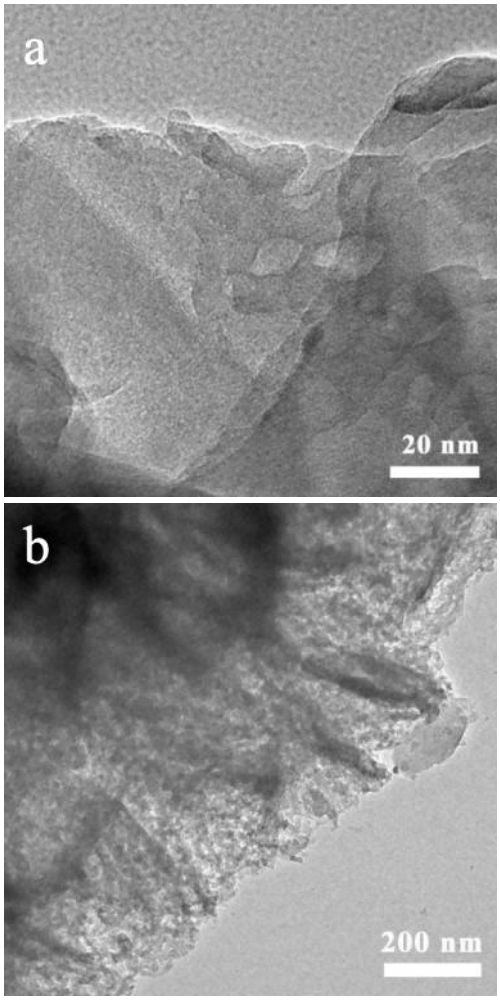

Figure S8. TEM images of g-C_3N_4. **a** 20nm, **b** 200 nm.

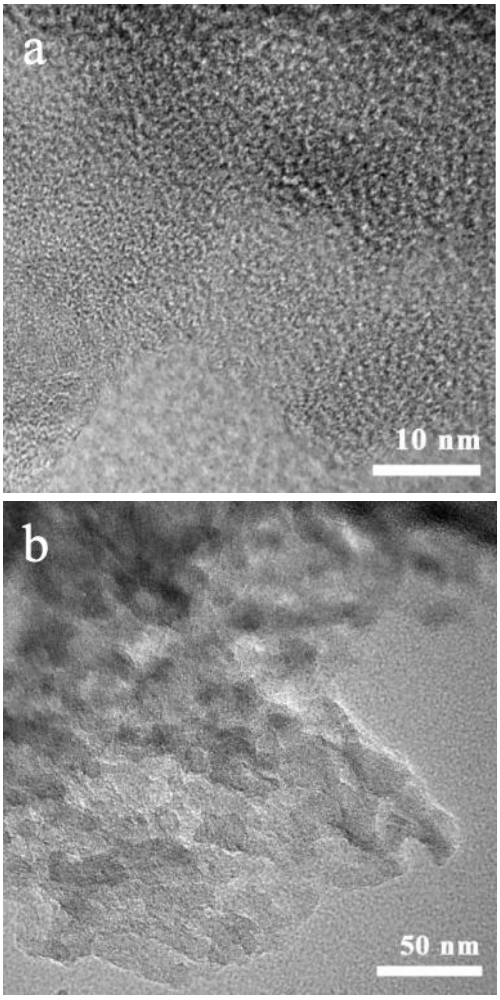

Figure S9. TEM images of COF@g-C_3N_4-0.2. **a** 10nm, **b** 50 nm.

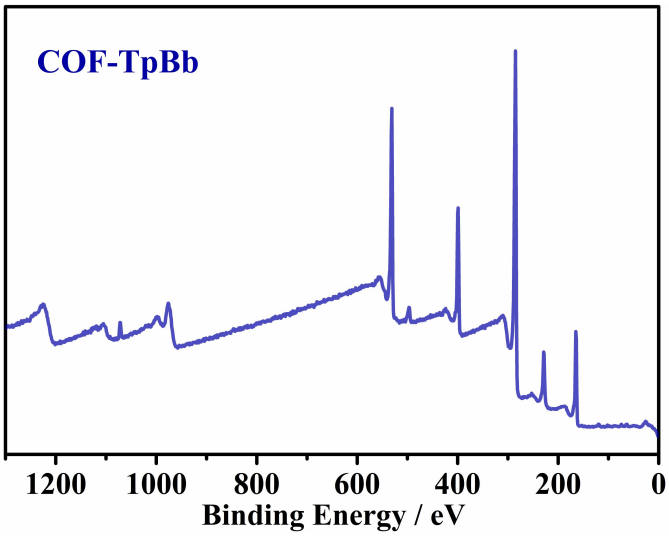

Figure S10. The XPS fitting of all elements of COF-TpBb.

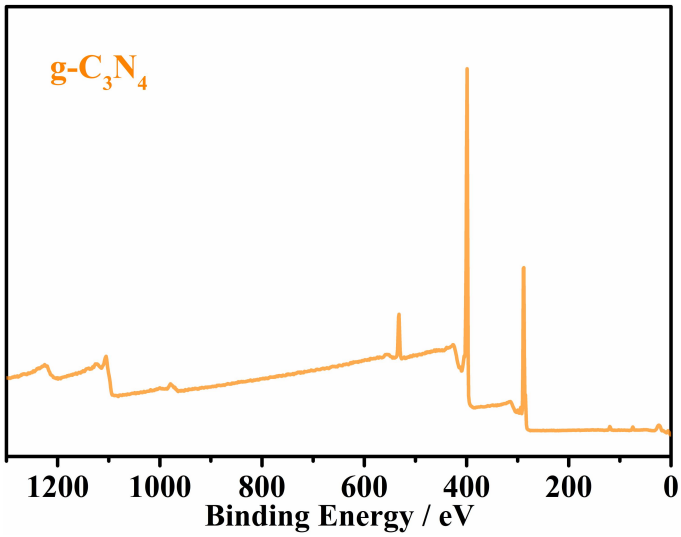

Figure S11. The XPS fitting of all elements of g-C_3N_4.

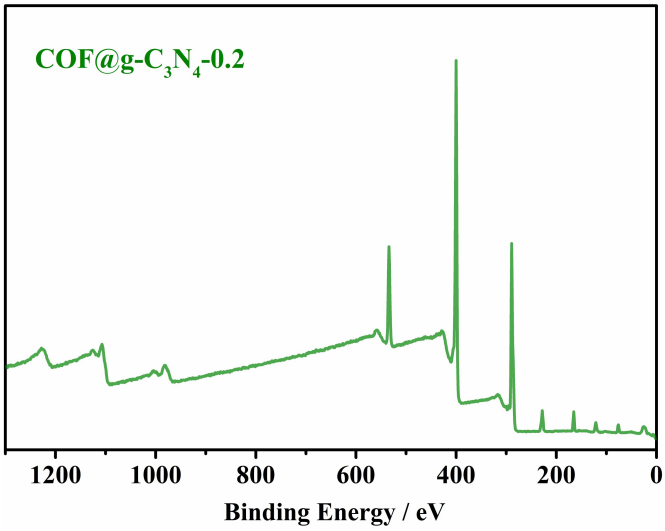

Figure S12. The XPS fitting of all elements of COF@g-C_3N_4-0.2.

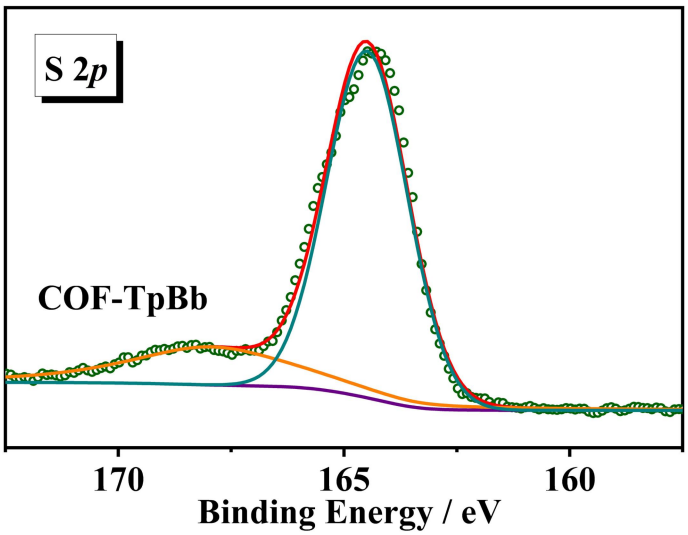

Figure S13. X-ray photoelectron spectroscopy (XPS) of S 2p for COF-TpBb.

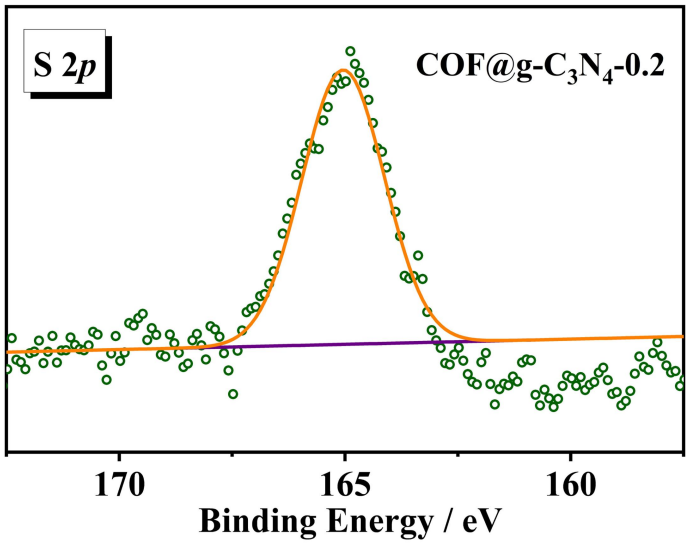

Figure S14. X-ray photoelectron spectroscopy (XPS) of S 2p for COF@g-C_3N_4-0.2.

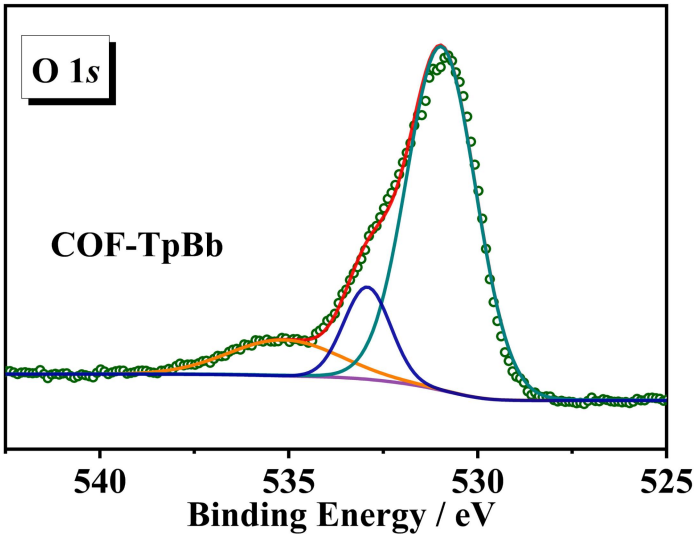

Figure S15. X-ray photoelectron spectroscopy (XPS) of O 1s for COF-TpBb.

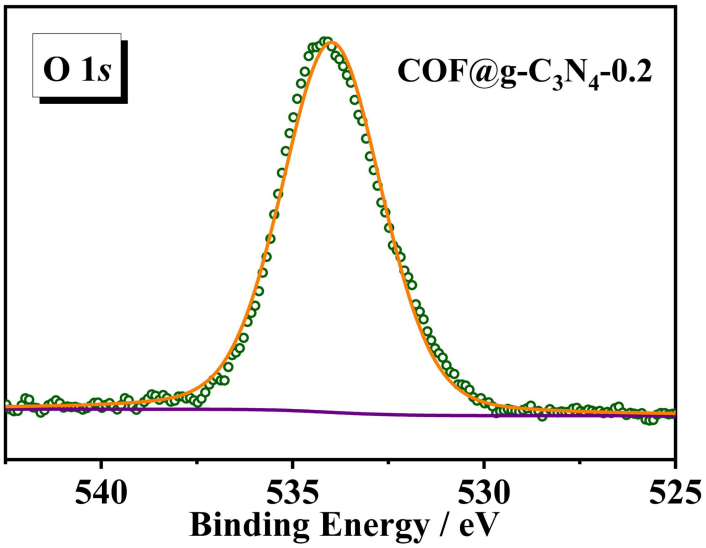

Figure S16. X-ray photoelectron spectroscopy (XPS) of O 1s for COF@g-C_3N_4-0.2.

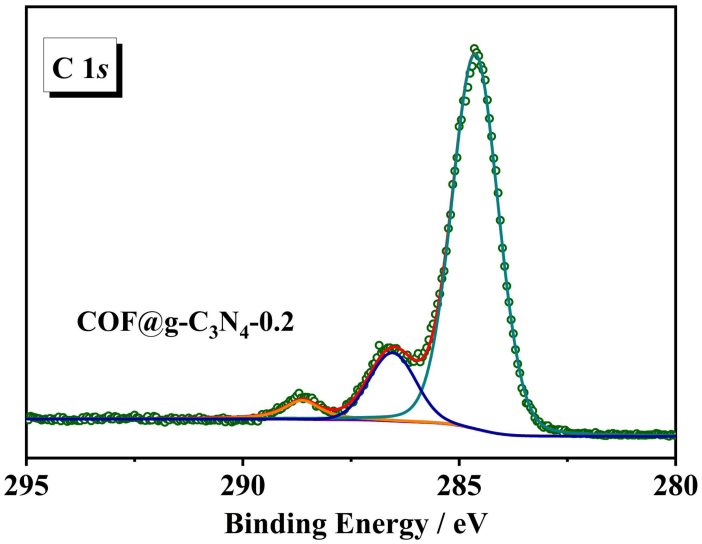

Figure S17. X-ray photoelectron spectroscopy (XPS) of C 1s for COF@g-C_3N_4-0.2.

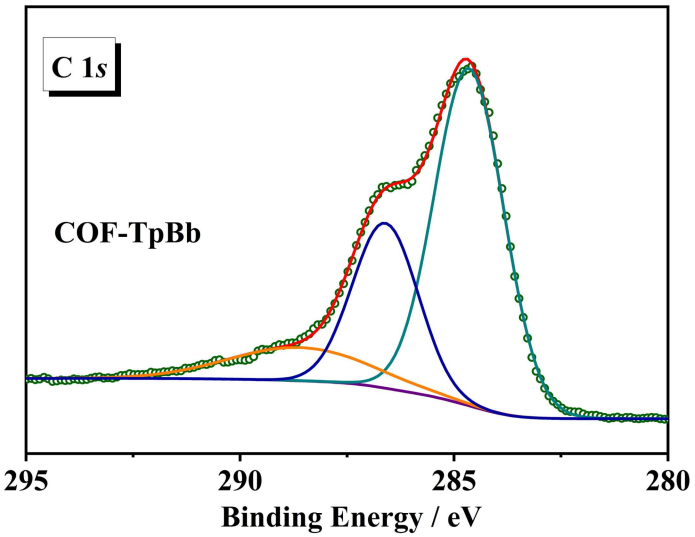

Figure S18. X-ray photoelectron spectroscopy (XPS) of C 1s for COF-TpBb.

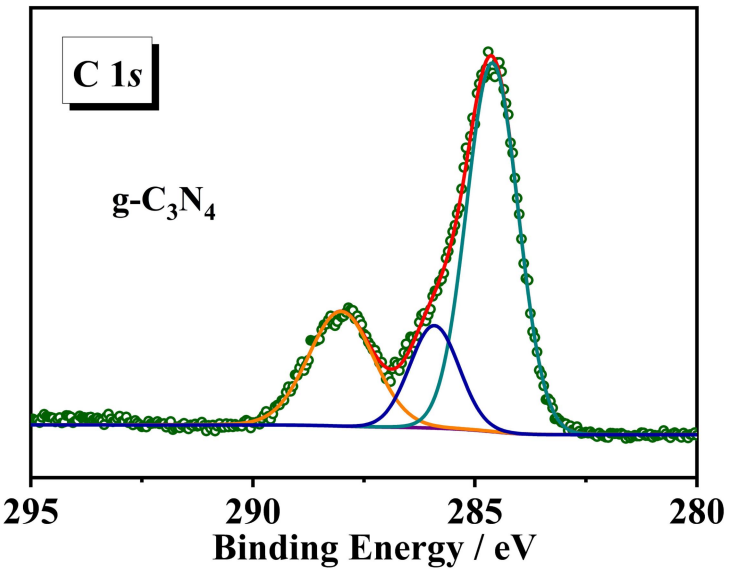

Figure S19. X-ray photoelectron spectroscopy (XPS) of C 1s for g-C_3N_4.

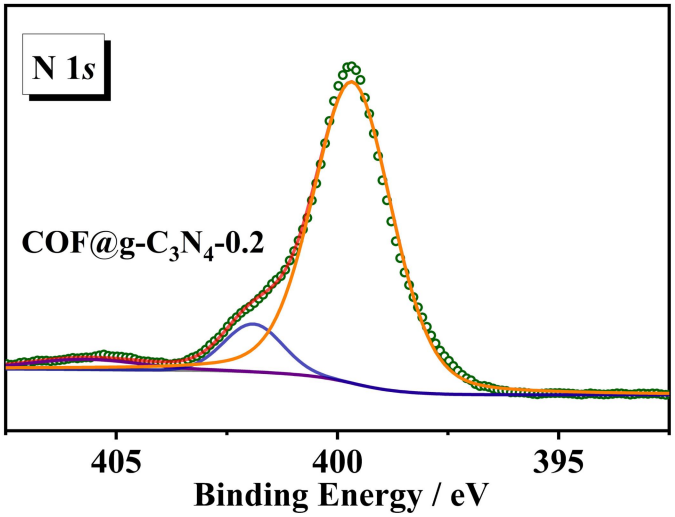

Figure S20. X-ray photoelectron spectroscopy (XPS) of N 1s for COF@g-C_3N_4-0.2.

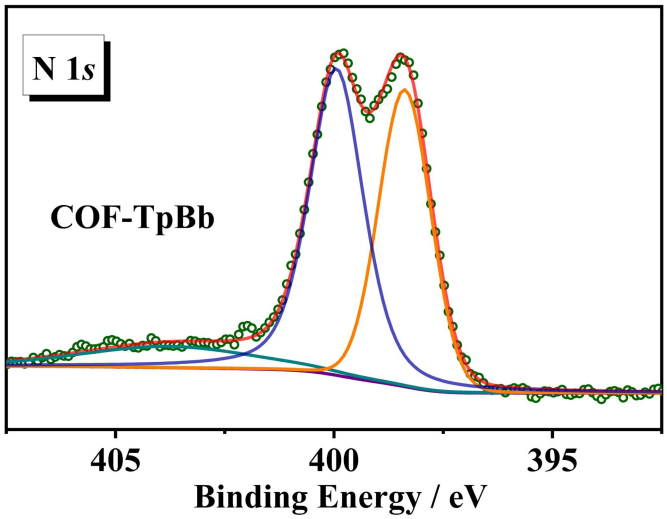

Figure S21. X-ray photoelectron spectroscopy (XPS) of N 1s for COF-TpBb.

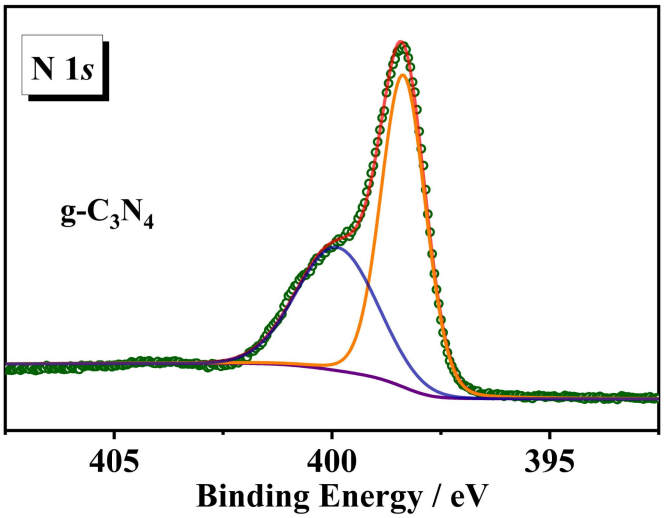

Figure S22. X-ray photoelectron spectroscopy (XPS) of N 1s for g-C_3N_4.

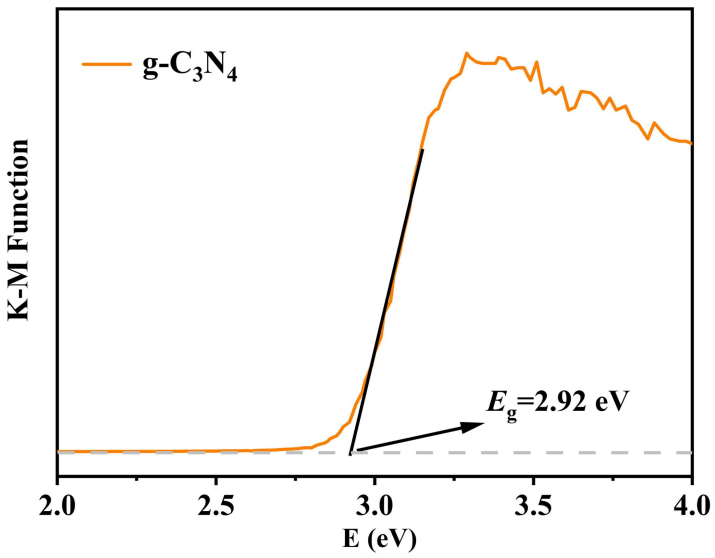

Figure S23. Tauc plot for g-C_3N_4.

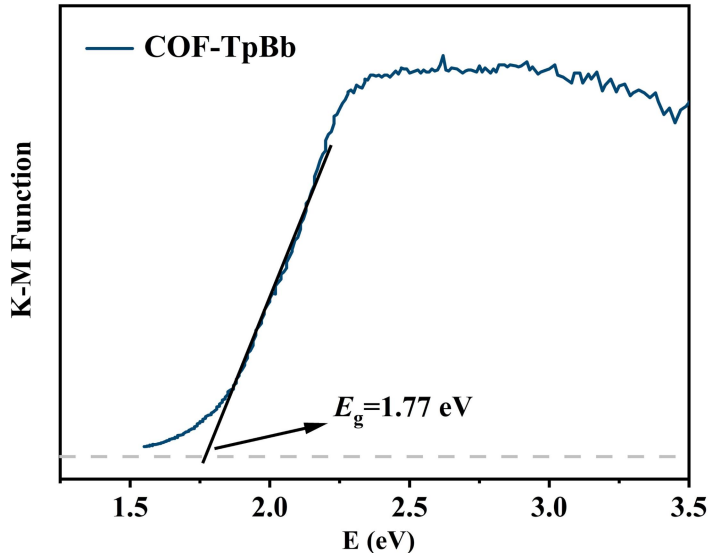

Figure S24. Tauc plot for COF-TpBb.

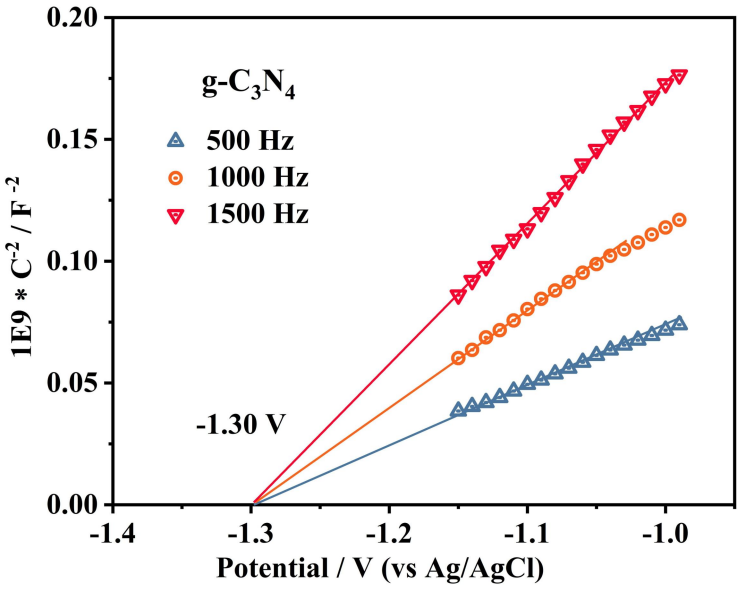

Figure S25. Mott-Schottky plots for g-C_3N_4 in 0.1 M Na_2SO_4 aqueous solution.

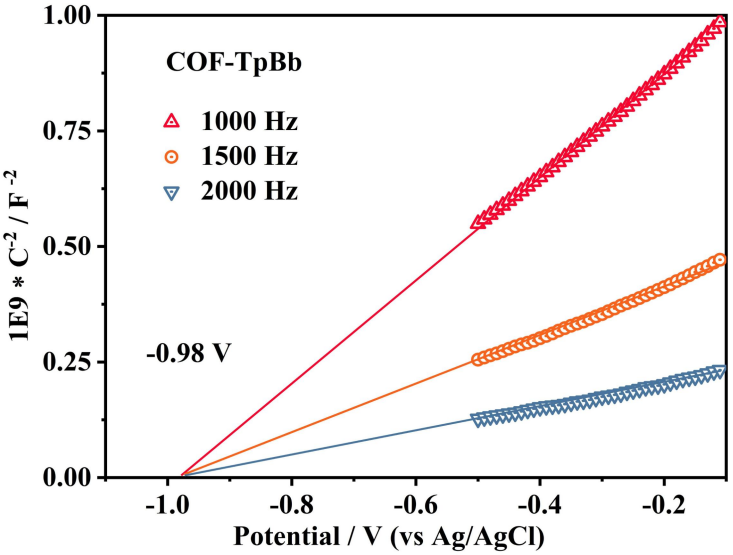

Figure S26. Mott-Schottky plots for COF-TpBb in 0.1 M Na_2SO_4 aqueous solution.

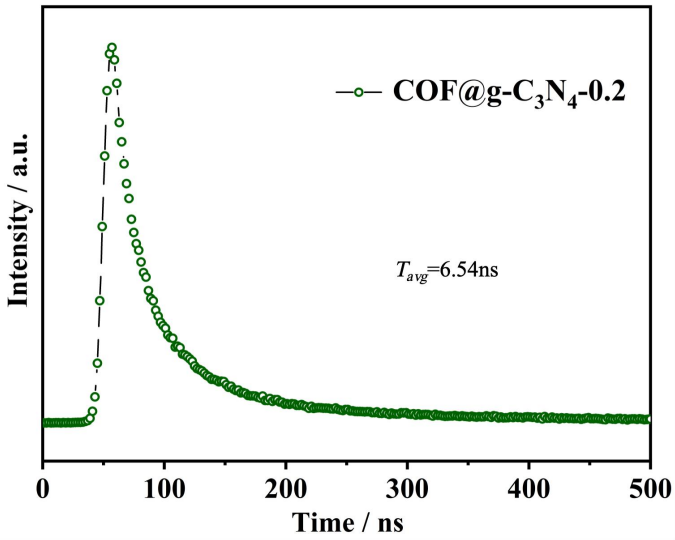

Figure S27. Time-resolved fluorescence decay spectroscopy of COF@g-C_3N_4-0.2.

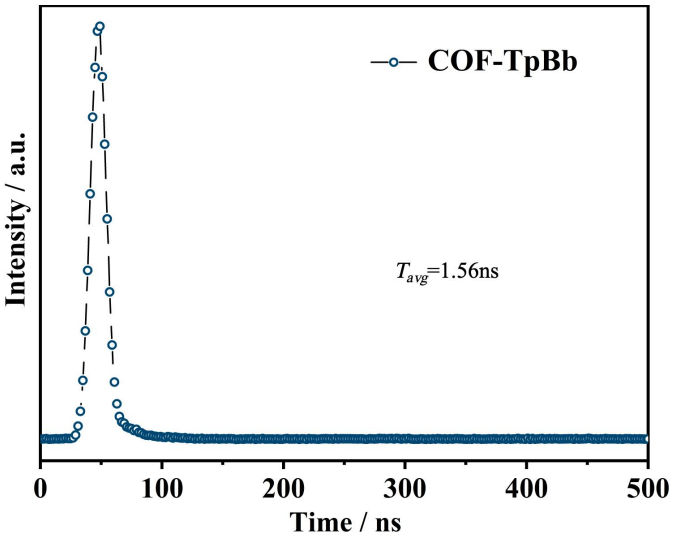

Figure S28. Time-resolved fluorescence decay spectroscopy of COF-TpBb.

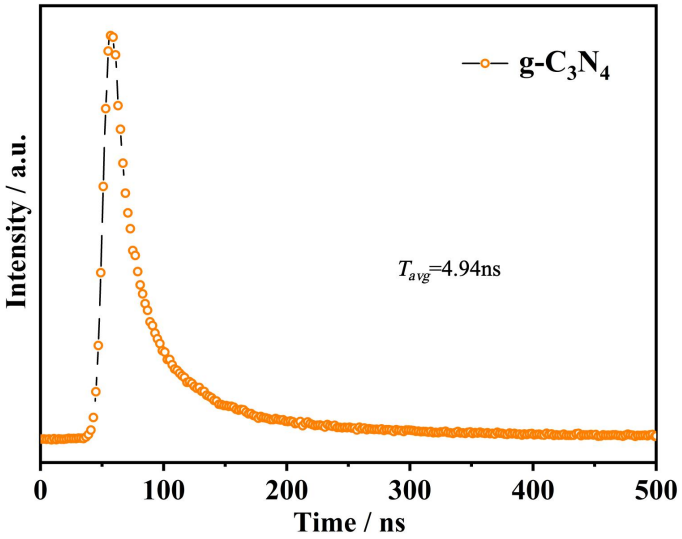

Figure S29. Time-resolved fluorescence decay spectroscopy of g-C_3N_4.

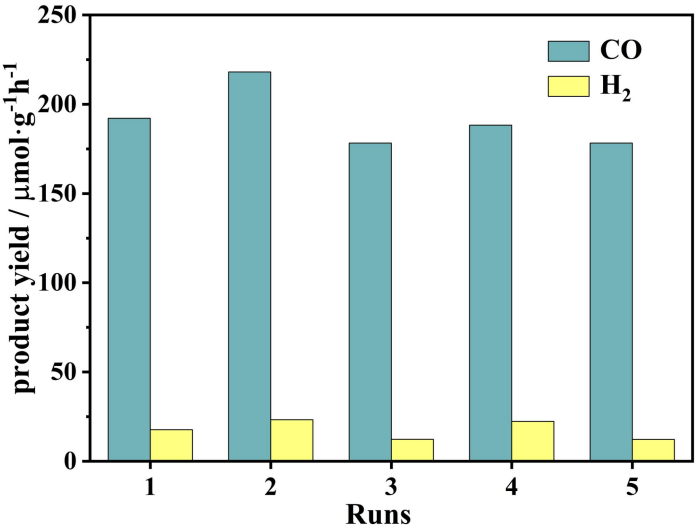

Figure S30. The yield of CO and H_2 with catalysis experiments of the same catalyst in different batches.

Table S1 Summary of related work based on g-C_3N_4 materials for photocatalytic CO_2 reduction

Photocatalyst	Solvent	PS	Light source	Products(CO)	Ref
$CuInS_2$/PCN	H_2O	TEOA	300 W Xe lamp	105.89 μmol·g^{-1}·h^{-1}	9
O/La-CN	MeCN	TEOA	300 W Xe lamp	92 μmol·g^{-1}·h^{-1}	10
Co_4@g-C_3N_4	MeCN	TEOA	300 W Xe lamp	89.6 μmol·g^{-1}·h^{-1}	11
CoOx/MCN	MeCN	TEOA	300 W Xe lamp	10.2 μmol·g^{-1}·h^{-1}	12
mpg-CNx| $CoPPc_{11.9}$	MeCN	TEOA	400 W Hg lamp	12.4 μmol·g^{-1}·h^{-1}	13
WO_3/g-C_3N_4	H_2O	TEOA	UV ($254 \leq \lambda < 420$nm)	58.41 μmol·g^{-1}·h^{-1}	14
g-C_3N_4@UIO66	MeCN	TEOA	300 W Xe lamp	9.9 μmol·g^{-1}·h^{-1}	15
ZIS/BCN-1	H_2O	TEOA	300 W Xe lamp	158 μmol·g^{-1}·h^{-1}	16
BA_{20} - CNS - PDA_{15}	MeCN	TEOA	LED （420nm < λ）	158 μmol·g^{-1}·h^{-1}	17
COF@g-C_3N_4-0.2	MeCN	TEOA	LED （420nm < λ）	195 μmol·g^{-1}·h^{-1}	This Work

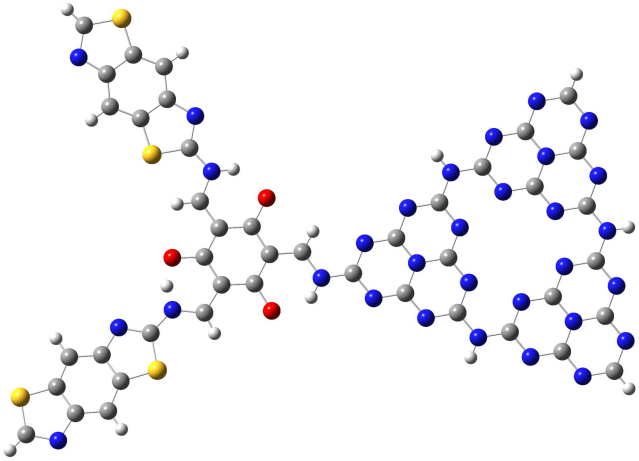

Figure S31. Computational model image for COF@g-C_3N_4 with a cluster model.

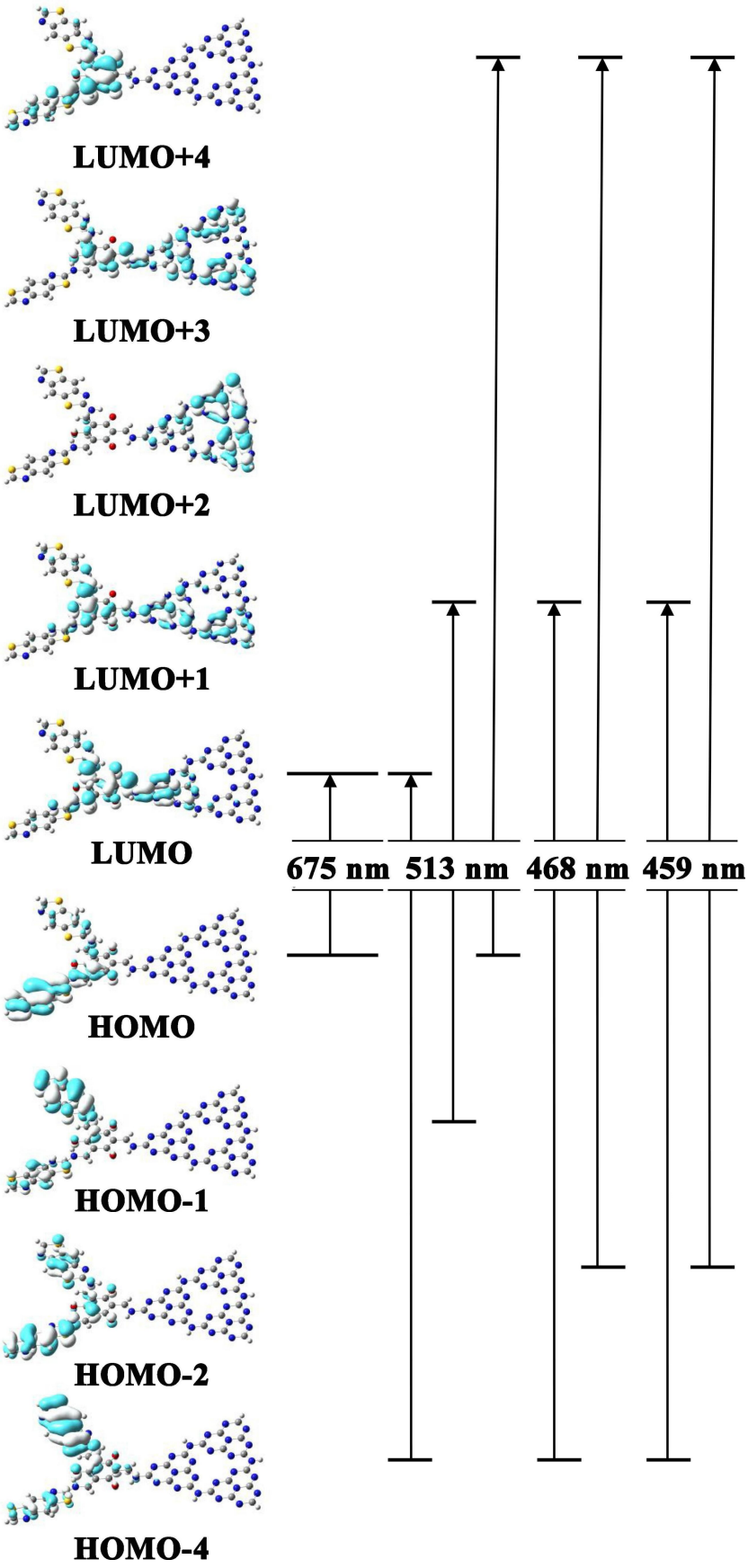

Figure S32. The molecular orbital composition analysis of COF@g-C_3N_4.

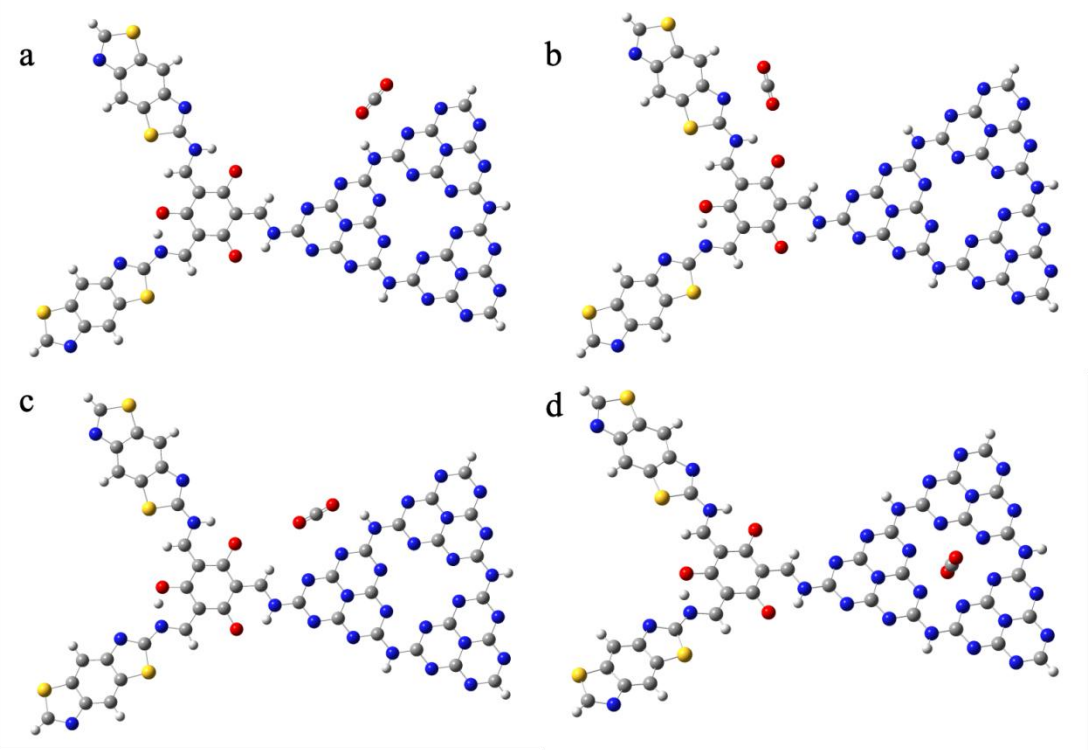

Figure S33. The model plots of CO_2 at adsorption sites **a,b,c,d** on COF@g-C_3N_4.([Cat.-CO_2]-a (-b, -c, -d)).

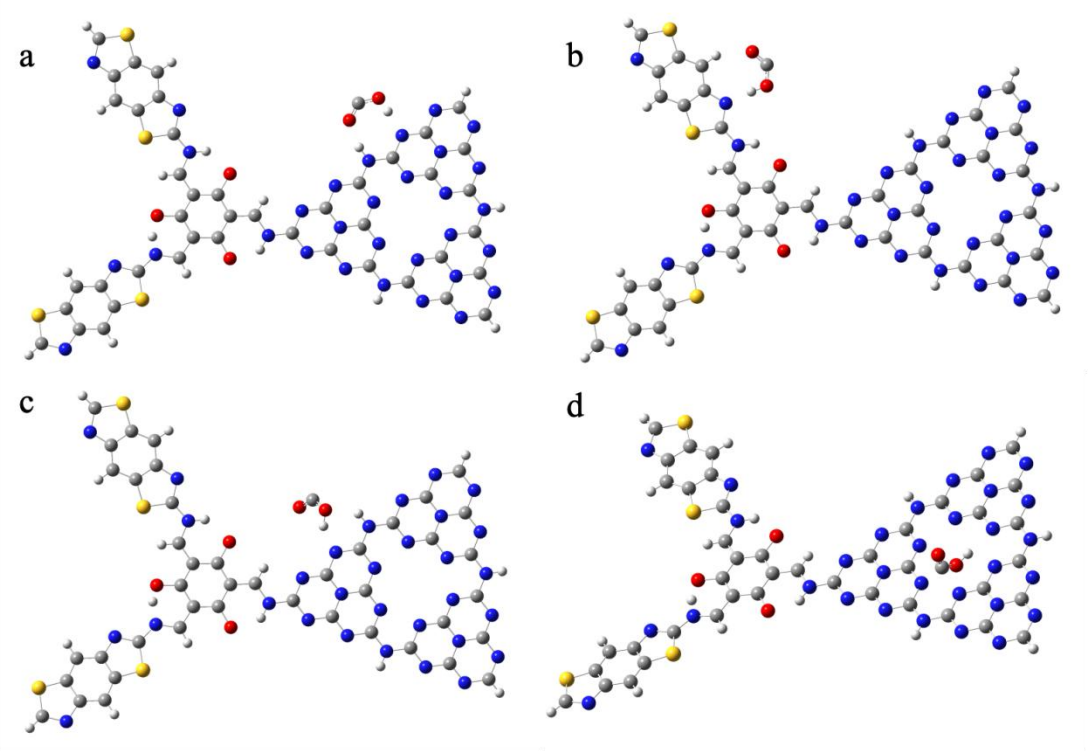

Figure S34. The model plots of -OCOH at adsorption sites **a,b,c,d** on COF@g-C_3N_4. ([Cat.-OCOH]-a (-b, -c, -d)).

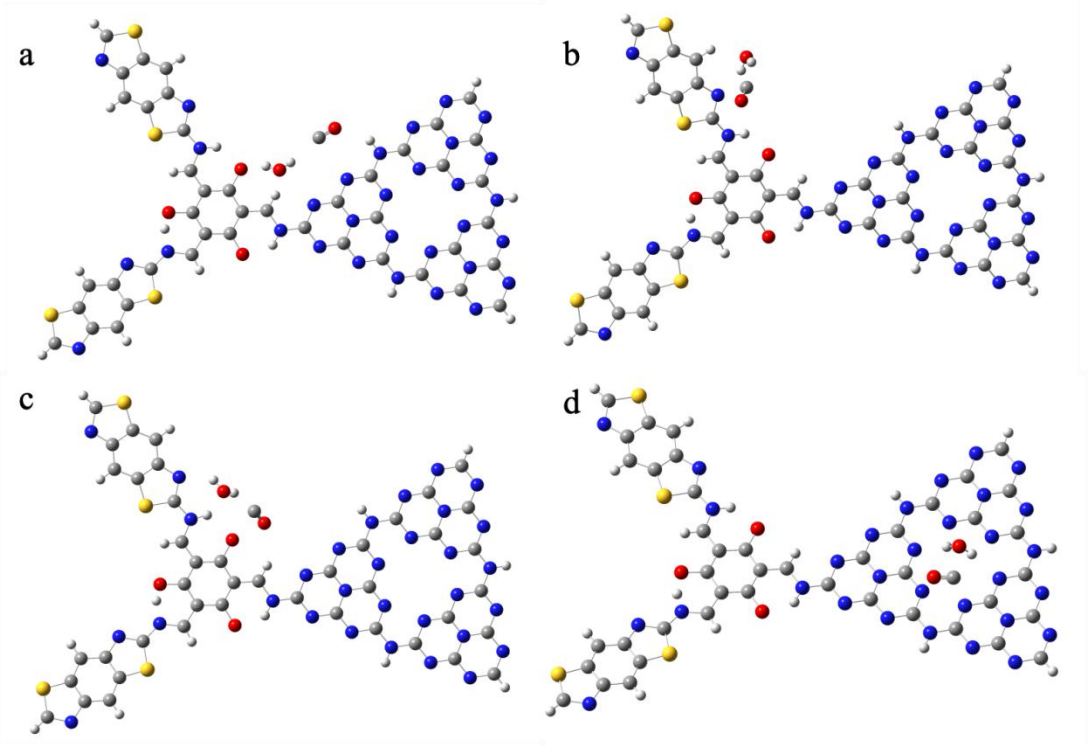

Figure S35. The model plots of -CO -H_2O at adsorption sites **a,b,c,d** on COF@g-C_3N_4.([Cat.-CO -H_2O]-a (-b, -c, -d)).

[1] M. Lu, M. Zhang, J. Liu, T. Y. Yu, J. N. Chang, L. J. Shang, S. L. Li, Y. Q. Lan, *J. Am. Chem. Soc.* 2022, **144**, 1861-1871.

[2] F.-M. Zhang, J.-L. Sheng, Z.-D. Yang, X.-J. Sun, H.-L. Tang, M. Lu, H. Dong, F.-C. Shen, J. Liu, Y.-Q. Lan, *Angew. Chem. Int. Ed.* 2018, **57**, 12106-12110.

[3] J.-X. Cui, L.-J. Wang, L. Feng, B. Meng, Z.-Y. Zhou, Z.-M. Su, K. Wang, S. Liu, *J. Mater. Chem. A* 2021, **9**, 24895-24902.

[4] H. Zhong, R. J. Sa, H. W. Lv, S. L. Yang, D. Q. Yuan, X. C. Wang, R. H. Wang, *Adv. Funct. Mater.*, 2020, **30**, 2002654.

[5] J. Zhou, W. C. Chen, C. Y. Sun, L. Han, C. Qin, M. M. Chen, X. L. Wang, E. B. Wang, Z. M. Su, *J. Mater. Chem. A*, 2018, **6**, 21596.

[6] J. Wang, H.-Y. Tan, Y. Zhu, H. Chu, H. M. Chen, *Angew. Chem. Int. Ed.* 2021, **60**, 17254-17267.

[7] K. Kobayashi, T. Kikuchi, S. Kitagawa, K. Tanaka, *Angew. Chem. Int. Ed.* 2014, **53,** 11813-11817.

[8] H.-Q. Xu, J. Hu, D. Wang, Z. Li, Q. Zhang, Y. Luo, S.-H. Yu, H.-L. Jiang, *J. Am. Chem. Soc.* 2015, **137**, 13440-13443.

[9] K. Yang, J. Yang, Y. Yesire, K. Zhong, P. Yan, H. Liu, H. Li, Y. Song, M. He and H. Xu, *Sep. Purif. Technol.*, 2024, **341**, 126808.

[10] P. Chen, B. Lei, X. a. Dong, H. Wang, J. Sheng, W. Cui, J. Li, Y. Sun, Z. Wang and F. Dong, *ACS Nano*, 2020, **14**, 15841-15852.

[11] J. Zhou, W. Chen, C. Sun, L. Han, C. Qin, M. Chen, X. Wang, E. Wang and Z. Su, *ACS Appl. Mater. Inter.*, 2017, **9**, 11689-11695.

[12] J. Lin, Z. Pan and X. Wang, *ACS Sustain. Chem. Eng.*, 2014, **2**, 353-358.

[13] C. Cometto, R. Kuriki, L. Chen, K. Maeda, T.-C. Lau, O. Ishitani and M. Robert, *J. Am. Chem. Soc.*, 2018, **140**, 7437-7440.

[14] X. Li, X. Song, C. Ma, Y. Cheng, D. Shen, S. Zhang, W. Liu, P. Huo and H. Wang, *ACS Appl. Nano Mater.*, 2020, **3**, 1298-1306.

[15] L. Shi, T. Wang, H. Zhang, K. Chang and J. Ye, *Adv. Funct. Mater.*, 2015, **25**, 5360-5367.

[16] K. Y. Kumar, L. Parashuram, M. K. Prashanth, H. Shanavaz, C. B. P. Kumar, V. S. A. Devi, F. Alharethy, B.-H. Jeon and M. S. Raghu, *J. Environ. Chem. Eng.*, 2023, **11**, 110867.

[17] M. Li, S. Zhang, X. Liu, J. Han, X. Zhu, Q. Ge and H. Wang, *Eur. J. Inorg. Chem.*, 2019, **2019**, 2058-2064.

[18] M. Gao, L. Sun, C. Ma, X. Li, H. Jiang, D. Shen, H. Wang and P. Huo, *Inorg. Chem.*, 2021, **60**, 1755-1766.

[19] J. Yang, X. Zhu, Z. Mo, J. Yi, J. Yan, J. Deng, Y. Xu, Y. She, J. Qian, H. Xu and H. Li, *Inorg. Chem. Front.*, 2018, **5**, 3163-3169.